University of Glasgow

DEPARTMENT OF

AEROSPACE ENGINEERING

The Application of an Unfactored Method to the Simulation of Nonlinear Aerofoil Responses: Part I - Verification for Inviscid Flows

K.J. Badcock and G.Sim

Glasgow University Aero report 9432

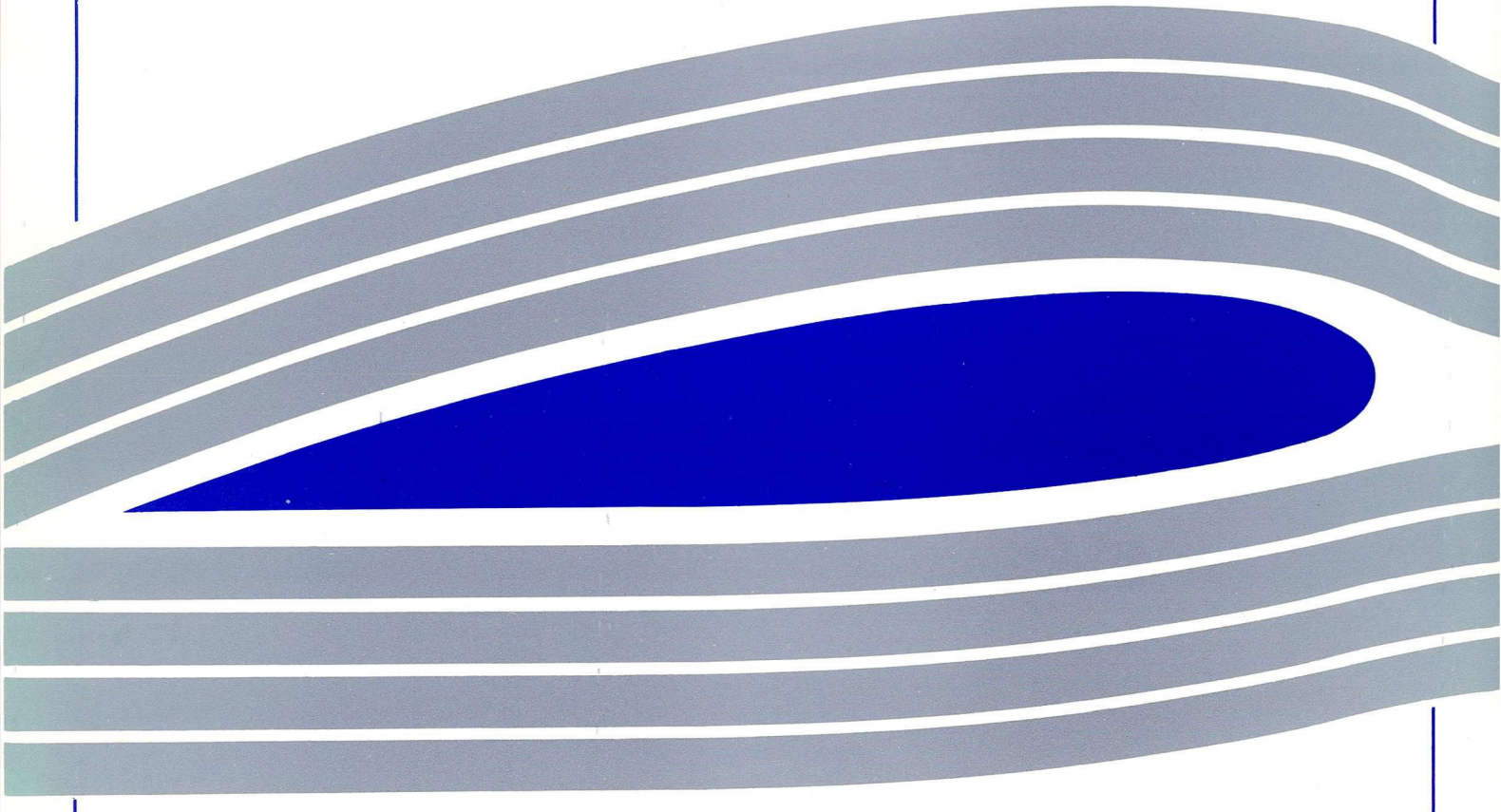

The Application of an Unfactored Method to the Simulation of Nonlinear Aerofoil Responses: Part I - Verification for Inviscid Flows

K.J. Badcock and G.Sim

Glasgow University Aero report 9432

The Application of an Unfactored Method to the Simulation of Nonlinear Aerofoil Response: Part I - Verification for Inviscid Flows

K.J. Badcock and G.Sim [1]

Abstract. An unfactored solution method developed for the Navier-Stokes equations is applied to study the nonlinear aeroelastic response of an aerofoil. A loosely coupled approach is adopted with the structural equations and the flow equations being solved in sequence. The flow solver efficiency is compared with the standard ADI method and the results are compared with previous computations for the NACA64A006 aerofoil.

1 Introduction

A fundamental problem of aerospace engineering is to determine the motion of a vehicle released into a flow. For some flow conditions, the fluid-structure interaction can have terminal consequences for the flight vehicle and hence this interaction must be investigated in detail during the design stage. Computational tools have a major role to play in this process due to the expense of flutter wind tunnel tests.

A hierachy of flow models exists which can describe increasingly complicated flow features. For general flutter calculations, the capability to model shock waves and flow separation is important because of the influence these features can have on the structural response. Examples include the flutter dip in the transonic regime and vortex induced instabilities. Therefore, the appropriate level of modelling for general flutter calculations is the Navier-Stokes equations. However, the computational cost of solving these equations at present precludes their routine use in the flutter analysis of complex flight vehicles.

The present work is aimed at providing efficient methods for solving the unsteady Navier-Stokes equations with application to the aeroelastic problem. A method for unsteady and turbulent aerofoil flows was developed in [6] [7]. Evaluation and verification of this method was achieved by application to standard AGARD aeroelastic pitching aerofoil test flows.

This method was first coupled with general aeroelastic structural subroutines as a feasability study for the more complicated three-dimensional case. The flow solver was also coupled with a much simpler code written specifically to solve the equations of motion describing an aerofoil which is free to move in pitch and plunge. Numerical tests are presented and comparison is made with previous computational results [5] to verify this second coupled code for several nonlinear aeroelastic responses.

[1] Department of Aerospace Engineering, University of Glasgow, Glasgow, G12 8QQ, UK

Glasgow University Aerospace Engineering Report 9432.

2 AF-CGS Method

The two-dimensional thin-layer Navier-Stokes equations in generalised co-ordinates are given by

$$\frac{\partial \mathrm{w}}{\partial t} + \frac{\partial \mathrm{f}}{\partial \xi} + \frac{\partial \mathrm{g}}{\partial \eta} = (Re)^{-1} \frac{\partial \mathrm{s}}{\partial \xi} \tag{1}$$

where

$$\mathrm{w} = J^{-1} \begin{bmatrix} \rho \\ \rho u \\ \rho v \\ e \end{bmatrix}, \mathrm{f} = J^{-1} \begin{bmatrix} \rho U \\ \rho u U + \xi_x p \\ \rho v U + \xi_y p \\ U(e+p) - \xi_t p \end{bmatrix},$$

$$\mathrm{g} = J^{-1} \begin{bmatrix} \rho V \\ \rho u V + \eta_x p \\ \rho v V + \eta_y p \\ V(e+p) - \eta_t p \end{bmatrix},$$

$$\mathrm{s} = J^{-1} \begin{bmatrix} 0 \\ \mu m_1 u_\xi + (\mu/3) m_2 \xi_x \\ \mu m_1 v_\xi + (\mu/3) m_2 \xi_y \\ \mu m_1 m_3 + (\mu/3) m_2 (\xi_x u + \xi_y v) \end{bmatrix}.$$

Here,

$$U = \xi_t + \xi_x u + \xi_x v$$

$$V = \eta_t + \eta_x u + \eta_x v$$

$$m_1 = \xi_x^2 + \xi_y^2$$

$$m_2 = \eta_x^2 + \eta_y^2$$

$$m_3 = (u^2 + v^2)/2 + Pr^{-1}(\gamma - 1)^{-1}(c^2)_\xi$$

and J is the determinant of the Jacobian of the transformation $x = x(\xi, \eta, t)$ and $y = y(\xi, \eta, t)$. Here ρ, u, v, e, p, Pr, Re, c, γ denote

density, the two components of velocity, energy, pressure, the Prandtl number, the Reynolds number, the speed of sound and the constant ratio of the specific heats respectively. The viscosity is composed of a part due to the natural viscosity of the fluid and a term to account for turbulence. Sutherland's law is used to describe the variation of the fluid viscosity with temperature. The Baldwin-Lomax model is used to provide a value for the turbulent viscosity.

A finite volume scheme is used to solve this system. Osher's method is used for the convective terms in the formulation for curvilinear coordinates as given in [11]. A MUSCL interpolation is used to provide second or third order accuracy and the Von Albada limiter prevents spurious oscillations from occuring around shock waves. Central differencing is employed for the viscous terms.

Implicit solution methods are generally prefered for viscous calculations due to the severe stability limits inherent in explicit methods. One implicit step can be written as

$$(I + \Delta t\frac{\partial R_\xi}{\partial w} + \Delta t\frac{\partial R_\eta}{\partial w})\delta w = -\Delta t(R_\xi + R_\eta) \qquad (2)$$

where

$$\frac{\partial(f)}{\partial \xi} \approx R_\xi$$

$$\frac{\partial(g-s)}{\partial \eta} \approx R_\eta.$$

The alternating direction implicit (ADI) form of this method is obtained by replacing the left hand side of (2) by the factored form

$$(I + \Delta t\frac{\partial R_\xi}{\partial w} + \Delta t\frac{\partial R_\eta}{\partial w}) \approx (I + \Delta t\frac{\partial R_\xi}{\partial w})(I + \Delta t\frac{\partial R_\eta}{\partial w}). \quad (3)$$

The present method uses an unfactored solution of 2 by the Conjugate Gradient Squared iterative algorithm together with preconditioning based on the ADI factorisation given by equation 3. In general, this more accurate solution of the linear system allows larger time steps to be taken, thus reducing the overall work required to compute the evolution of the flow. A full discussion of this method can be found in [6].

The method described above was developed for the simulation of turbulent flows. However, in the present report we concentrate on inviscid results to allow comparison of results with a previous computational study. The inviscid flow solver is derived from the viscous one by neglecting viscous terms and ammending the *no-slip* wall boundary condition to one of *no-flow through* a solid boundary.

3 Structural Equations

The equations describing the motion of an aerofoil free to move in pitch and plunge are

$$\mathrm{M}\frac{d^2\mathrm{q}}{dt^2} + \mathrm{Kq} = \mathrm{F} \qquad (4)$$

where

$$\mathrm{q} = \begin{bmatrix} h/b \\ \alpha \end{bmatrix}, \mathrm{M} = \beta \begin{bmatrix} 1 & x_\alpha \\ x_\alpha & r_\alpha^2 \end{bmatrix},$$

$$\mathrm{K} = \beta \begin{bmatrix} \omega_R^2 & 0 \\ 0 & r_\alpha^2 \end{bmatrix}, \mathrm{F} = \begin{bmatrix} -C_L \\ 2C_M \end{bmatrix}.$$

Here, h is the aerofoil displacement in plunge which is positive downwards, b is the semi-chord, α is the aerofoil incidence, $\omega_R = \omega_h/\omega_\alpha$ is the ratio of the natural frequencies of plunging to pitching, x_α is the offset of the centre of gravity from the elastic axis, r_α is the radius of gyration, C_L is the lift coefficient and C_M is the moment coefficient about the elastic axis. The constant β is given by

$$\beta = \frac{4}{\pi \mu \omega_\alpha^R}$$

where μ is the aerofoil to fluid mass ratio $m/\pi\rho_\infty b^2$ and ω_α^R is the natural frequency of pitching non-dimensionalised by $U_\infty/2b$ where U_∞ is the free stream fluid speed. A reduced velocity for the problem which is convenient for expressing the results can be defined as $\overline{U} = 2/\omega_\alpha^R$.

Equation (4) is standard for any aeroelastic analysis of a pitching and plunging aerofoil. Linear aerodynamic theory can be used to yield the forces on the right hand side of 4. However, for flow conditions where shock waves or separation are present, the nonlinear interaction between the flow and the aerofoil motion needs to be modelled. For this type of flow the general model is the Navier-Stokes equations. In the present work the method described above for solving these flow equations is coupled with a solution of equation (4) in the loose way depicted in figure 1. The flow solution is used to provide the forces needed to calculate the aerofoil motion; this motion is used to provide boundary conditions and the new geometry for the flow solution and so on.

At each time step the mesh needs to be adjusted to conform with the moving aerofoil. One way of doing this is to regenerate at each time step using a transfinite interpolation method with the outer boundary remaining fixed and the aerofoil position changing (see [2]). For the pitching and plunging problems studied in this paper it is sufficient to move the mesh rigidly with the aerofoil. However, regeneration allows more generality with the potential to tackle aerofoils with flaps and problems with more complex geometries using the multi-block approach. Some care is required with the calculation of cell areas, with spatial conservation being violated if simple geometric relations are used. For most published aeroelastic studies this point has been neglected (eg [10]) but this assumption should be investigated further because the motivation behind using an unfactored method is to allow the use of large time steps and this is in conflict with neglecting spatial conservation. Hence, in the present report we use mesh rotation to avoid this difficulty.

The structural equations have been solved in two ways. The first was by a set of subroutines for general aeroelastic analysis provided by British Aerospace [9]. This was done as a feasability and familiarisation study for coupling these subroutines with a three-dimensional flow solver. Secondly, a three stage Runge-Kutta solver was implemented specifically for the solution of equation (4) and it is this code, specific

to the two-degree-of-freedom motion of an aerofoil, which is used for the results presented herein. In both cases, the time step for the coupled solution is determined by the flow solver.

4 Results for NACA64A006 Aerofoil

The nonlinear aeroelastic stability of a NACA64A006 aerofoil is now considered. This problem was studied in some detail in [5] where a coupled Euler-structural solution was used. The structural parameters are as given in [5]:

$$a=0.2$$

$$x_\alpha=0.2$$

$$r_\alpha^2=0.29$$

$$\omega_R^2=0.11789$$

$$\mu=10.0.$$

For Mach numbers in the transonic regime the interaction of the shock wave motion with the aerofoil motion leads asymptotically to limit cycle behaviour after a bifurcation from the stable undisturbed state. In addition, different types of instability can interact and an example of this is flutter-divergence interaction. As a first step towards a study of the influence of viscous effects on these phenomena, we reproduce some of the nonlinear responses in inviscid flow to demonstrate the utility of the unfactored approach for aeroelastic problems and to determine the influence of numerical parameters on the response. The approach taken in the numerical tests was to freeze all of the parameters except one and then to test when the solution became fixed with respect to this parameter. The order in which the parameters were tested meant that the *converged solutions* for the time step and mesh refinement are in fact spurious. However, since the solution obtained is broadly similar to the genuine solution (i.e. it involves limit cycle oscillations of a similar period and amplitude), the validity of the conclusions is unaffected.

4.1 Temporal Refinement

The first numerical issue we consider is time accuracy. The AFCGS method was introduced to overcome factorisation error effects inherent in the ADI method and hence time accuracy is of considerable interest. The test conditions chosen were $\overline{U}$=2.2, Mach 0.92, mesh 80x30 and far field distance 10c. The pitch responses obtained for a variety of steps per pitching cycle are shown in figure 2 and good time accuracy is obtained with 150 steps/cycle. The AFCGS method can reproduce the limit cycle behaviour with only 30 steps/cycle although the amplitude of the oscillation is in error by a factor of two. ADI requires a minimum of 100 steps/cycle to produce any solution but manages to compute the solution accurately with 150 steps/cycle. Hence, for the current inviscid problem there is no advantage in using the AFCGS method except for the increased robustness that is demonstrated by the ability to use large time steps. However, for the corresponding viscous problem it has been observed that the restriction on ADI is more severe with 300 steps/cycle required to obtain a solution whereas AFCGS can solve the problem with only 100 steps/cycle. This results in a fifty per cent improvement in turn around time by using AFCGS for the viscous problem. For an aeroelastic study a large number fo results are typically required and hence this represents a significant potential saving in CPU time.

4.2 Spatial Refinement

Next, we examine the effect of mesh refinement by fixing $\overline{U}$=2.2, the far field distance at 10c, the time step at 150 steps/cycle and the free stream Mach number at 0.92. The pitch response on various meshes is shown in figure 3. The converged response shows a doubly periodic behaviour which in fact turns out to be due to the proximity of the far field. Good spatial accuracy is obtained on the 150x30 mesh. The refinement in the streamwise direction is more important than in the normal direction, due to the importance of resolving the shock wave accurately for this problem.

The results of this report were obtained on meshes which remain fixed to the aerofoil i.e. they are rigidly rotated with the aerofoil. However, for generality, regeneration is more flexible since it allows for the possibility of fixed outer boundaries (important if a multiblock scheme is being used) and of aerofoil deformation or flap motion. If the cell areas are changing in time then extra errors are introduced into the calculation if these areas are calculated by a geometric relation and not by an extra partial differential equation related to the motion of the grid points (the global conservation law). This is a matter which requires further investigation before mesh regeneration can be used with confidence.

4.3 Far Field Location

The remaining numerical parameter to be considered is the far field location. The mesh size is fixed at 150x30, 150 steps/cycle are taken, $\overline{U}$=2.2 and the free stream Mach number is 0.92. The effect of varying the far field distance is shown in figure 4. It is clear that there is a qualitative difference between the result at a distance of 10c and at the larger distances. The doubly periodic behaviour dies away at the larger distances and it is concluded that a distance of 20c gives good accuracy. For later results at Mach 0.85 the doubly periodic behaviour is not observed at all for a far field at 20c.

The source of the doubly periodic behaviour remains unclear. It was shown in [1] that a far field distance of 10c was sufficient for an aerofoil flow at Mach 0.73 and subsequent experience has confirmed this. However, the far field distance required increases with the free stream Mach number [4]. It does not appear that the source of the modulation is spurious reflections from the far field since the frequency of the modulation does not depend on the far field distance. One problem with the numerical formulation is that the boundary flux is discontinuous when there is a change from inflow to

outflow or vice-versa. Despite this, the flux is differentiated. The switching will be particularly marked with mesh rotation. Further work is required to examine these points.

4.4 Comparison with Previous Results

Finally, we have arrived at a set of numerical parameters which give a reliable solution at Mach 0.92 and $\overline{U}$=2.2. Since the none of the time responses encountered for Mach numbers between 0.85 and 0.92 are more complicated than the limit cycle oscillations encountered at these conditions it is reasonable to assume that good accuracy can be obtained within this range by using the following numerical conditions:

- 150x30 mesh
- 150 steps/cycle
- far field distance of 20c.

These condtions were used to calculate the aerofoil response for varying $\overline{U}$ at a Mach number 0.92. The behaviour calculated in [5] showed a bifurcation to limit cycle oscillations at $\overline{U} \approx 2.0$ with the amplitude increasing with $\overline{U}$. Similar behaviour from the present results is shown in figure 5. The response has been found to be insensitive to the exact definition of the initial disturbance. In fact, the same asymptotic behaviour was observed when no disturbance was applied, with the aerofoil being *perturbed* by the small discrepancy between the starting solution and the exact steady state! At $\overline{U}$=2.0 the zero equilibrium is stable whereas limit cycles of increasing amplitude are observed for increasing $\overline{U} > 2.0$. The doubly periodic motion initially seen is more pronounced at the largest values of $\overline{U}$. The comparison of the computed amplitudes with those of [5] is shown in figure 7 and shows reasonable agreement. The discrepancies are presumably due to convergence questions relating to the numerical parameters since the numerical details differ for the two sets of results.

More varied behaviour is observed at Mach 0.85 where flutter divergence interaction is observed for a range of $\overline{U}$. This is illustrated in figure 6 and shows close qualitative agreement with the results of [5].The most interesting feature of these results is that both flutter and divergence are observed around the bifurcation point and that the limit cycle oscillations *kill off* the divergence.

It is important to note that the incidence is high for some of these cases and particularly at Mach 0.85. The Euler model certainly loses validity for some of these flows and hence it is important to repeat this study with a viscous flow model.

5 Conclusions

The capability of an unfactored method developed for the solution of the unsteady Navier-Stokes equations to calculate the nonlinear aeroelastic response of an aerofoil in inviscid flow has been demonstrated. A loosely coupled formulation with the structural solution was used and the mesh was regenerated at each time step by a fast algebraic method. Tests were carried out on flows featuring the NACA64A006 aerofoil which have been previously studied computationally by an Euler code. The limit cycle and flutter-divergence interaction behaviour which has previously been observed computationally was reproduced. An improvement in efficiency of 50 per cent was noted over the widely used ADI method. Care is necessary in elimininating numerical effects from the computed responses.

There is scope for further investigation of nonlinear responses in conjunction with theoretical work which is ongoing at Glasgow University. Initially this should be for inviscid flows but the study could then be repeated for turbulent flows to evaluate the influence of viscous effects. The code should be further verified by comparison with experimental pitch and plunge results available through the NASA benchmark program [3].

Work in three dimensions is under way [8] and this will include the coupling of the British Aerospace structural subroutines to a Navier-Stokes solver. Although the computing power available for this work has recently taken a quantum leap, with the designation of aeroelasticity as a part of the Grand Challenge problem of computational fluid dynamics leading to access to the Cray T3D at Edinburgh University, the CPU requirements for three-dimensional nonlinear aeroelasticity studies analogous to the present work in 2-D still exceeds current capabilities. However, with continuing improvement in computer power and numerical algorithms, this will not be the case for long. In the mean time, coupled 3-D Navier-Stokes codes will still be useful for identifying flutter boundaries in the transonic regime and also aeroelastic instabilities due to flow separation. However, this application does not make full use of the detailed flow information available. 2-D studies of nonlinear behaviour, in addition to their intrinsic interest, are useful to identify further applications for 3-D codes simulations of the future.

ACKNOWLEDGEMENTS

The first author was funded under EPSRC/MOD contract GR H 47371. The structural solution routines were implemented whilst the second author was on a Carnegie summer scholarship. The authors are grateful to Dr A.L. Gaitonde of Bristol University for providing the mesh generation subroutines, to Dr M.J. Knott of British Aerospace for providing structural solution subroutines and to Dr Knott and Dr J. Anderson of Glasgow University for their helpful comments on this work. Thre results presented were obtained on the intel iPSC i860 Hypercube located at the EPSRC Daresbury Laboratory.

REFERENCES

[1] K.J.Badcock B.Gribben and B.E.Richards, 'Far-field boundary conditions for Solutions to the Navier-Stokes equations', Technical report, G.U. Aero report 9324, (1993).

[2] A.L. Gaitonde and S.P. Fiddes, 'A moving mesh system for the calculation of unsteady flows', Technical report, A.I.A.A. 93-0641, (1993).

[3] R.M. Bennett M.H. Durham J.A. Rivera, B.E. Dansberry and W.A. Silva, 'NACA0012 benchmark model experimental flutter results with unsteady pressure distributions', Technical report, A.I.A.A. 92-2396-CP, (1992).

[4] J.L.Thomas and M.D.Salas, 'Far-field boundary conditions for transonic lifting solutions to the Euler equations', *A.I.A.A. J.*, **24**, 1074–1080, (1986).

[5] K.A.Kousen and O.O.Bendiksen, 'Nonlinear aspects of the transonic aeroelastic stability problem', in *29th Structures, Structural Dynamics and Materials Conference*. AIAA, (1988).

[6] K.J.Badcock, 'Computation of turbulent pitching aerofoil flows', Technical report, G.U. Aero report 9322, (1993).

[7] K.J.Badcock and A.L.Gaitonde, 'An unfactored method with moving meshes for solution of the Navier-Stokes equations for flows about aerofoils', *submitted for publication, August,1994*, (1994).

[8] K.J.Badcock and B.E.Richards, 'The simulation of transonic steady flows over wings', Technical report, G.U. Aero report 9430, (1994).

[9] M.J. Knott, 'The coupled solution of the unsteady aerodynamics and structual equations of motion in the time domain', Technical Report BAe-FAE-N-GEN-3752, British Aerospace, (1993).

[10] G.P. Guruswamy S. Obayashi and P.M. Goojian, 'Streamwise upwind algorithm for computing unsteady transonic flows past oscillating wings', *AIAA J.*, **29**, 1668–1677, (1991).

[11] S.Osher and S.R.Chakravarthy, 'Upwind schemes and boundary conditions with applications to Euler equations in general coordinates', *J. Comp. Phys.*, **50**, 447–481, (1983).

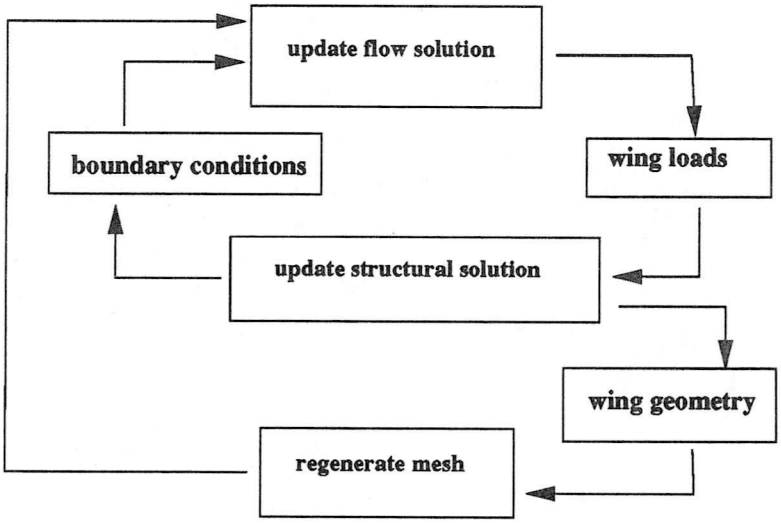

7

Figure 1. *Schematic diagram of the coupling between the flow solver and the structural solver.*

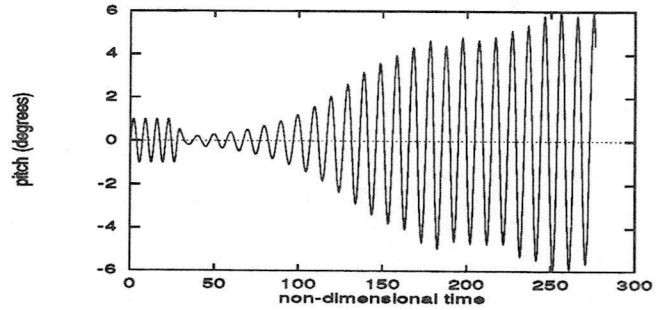

30 steps/cycle

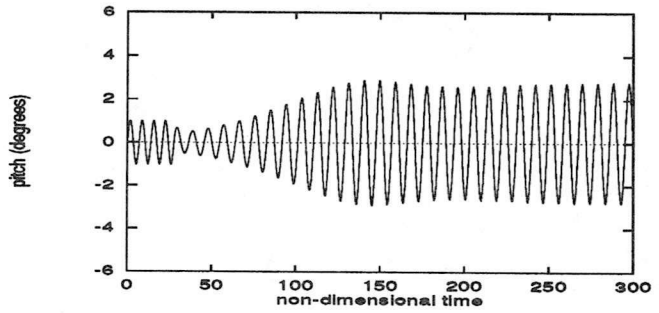

150 steps/cycle

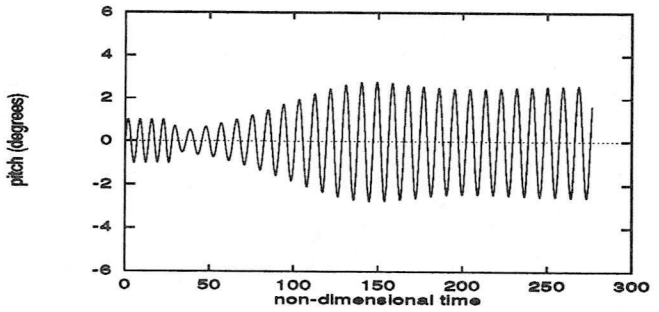

300 steps/cycle

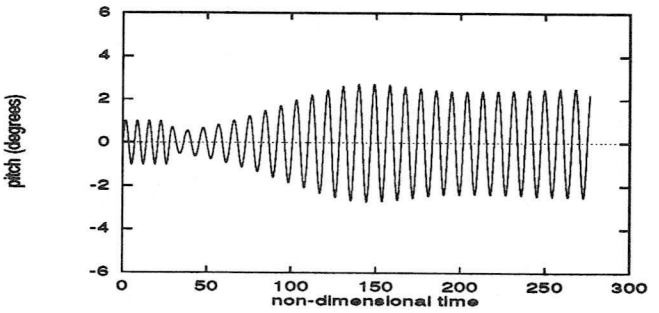

600 steps/cycle

Figure 2. *Time step refinement at Mach 0.92 and $\overline{U}$=2.2 on 80x30 mesh with far field distance 10c.*

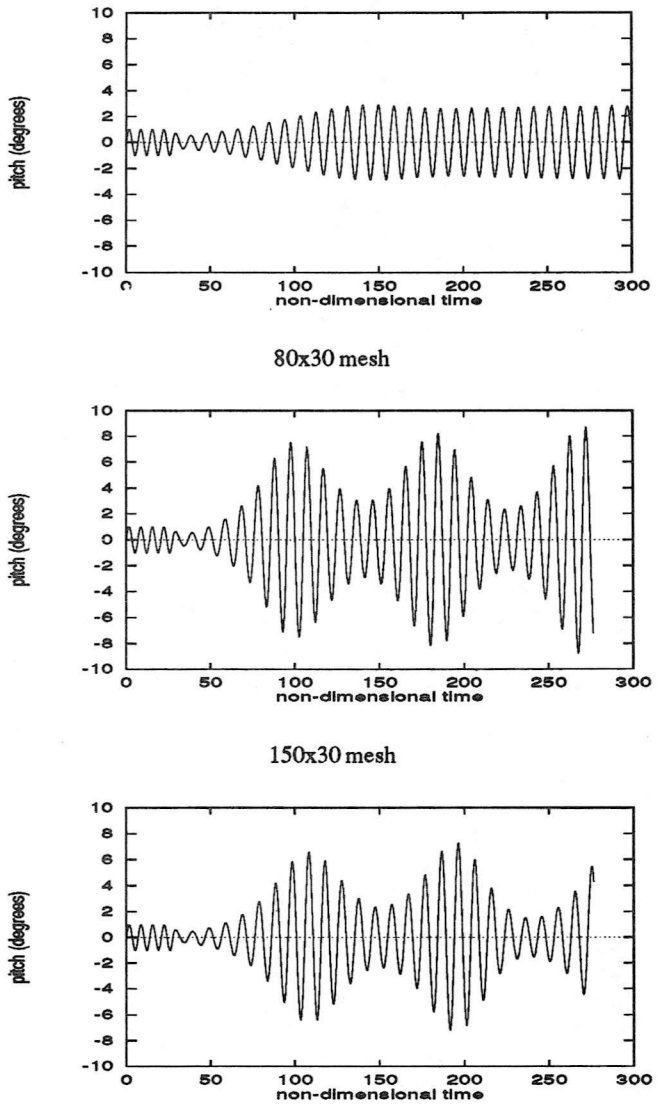

Figure 3. *Mesh refinement at Mach 0.92, $\overline{U}$=2.2, 150 steps per pitching cycle and far field distance 10c.*

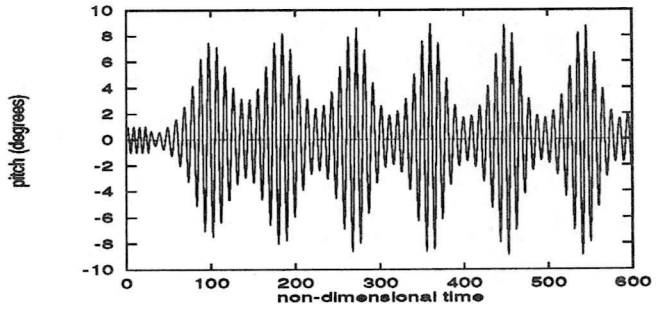

far field 10c

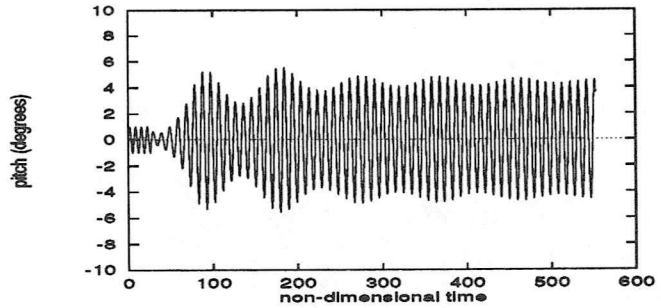

far field 20c

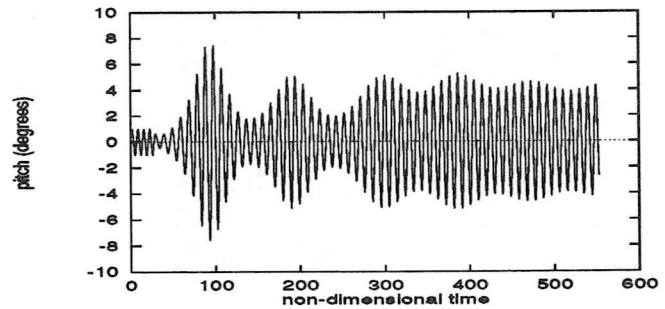

far field 40c

Figure 4. *Effect of far field distance at Mach 0.92, $\overline{U}$=2.2, 150x50 mesh and 150 steps per pitching cycle.*

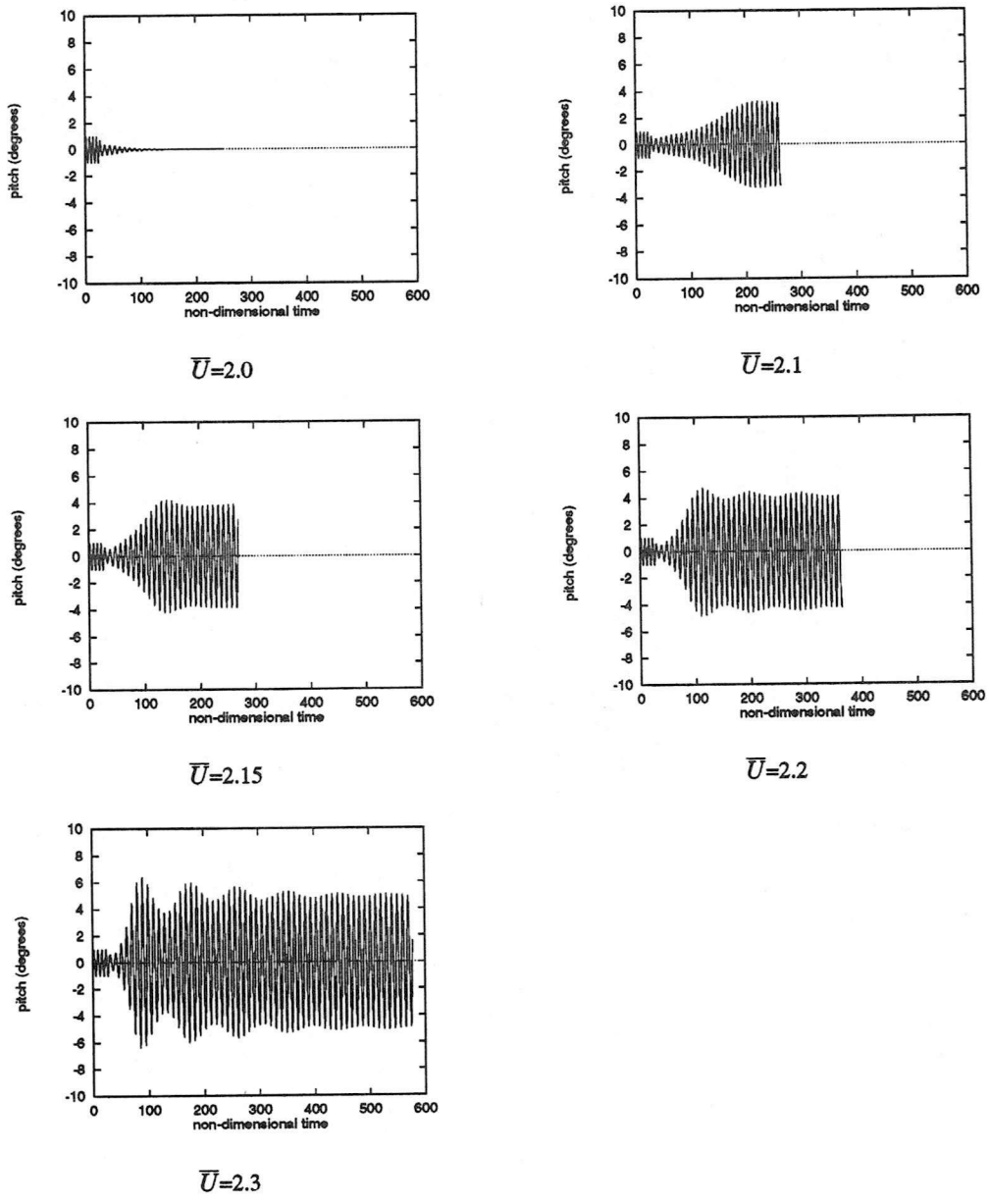

Figure 5. *Pitch response for varying $\overline{U}$ at Mach 0.92 on 150x30 mesh, far field at 20c and 150 steps/pitching cycle.*

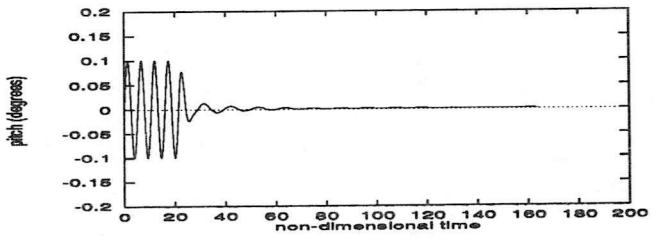

$\overline{U}$=1.7

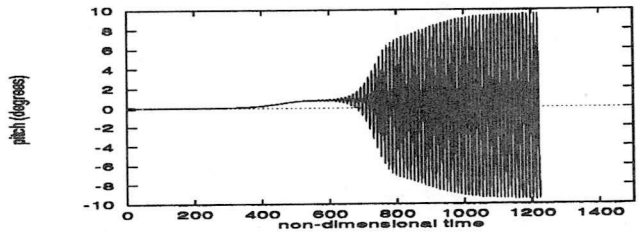

$\overline{U}$=1.95

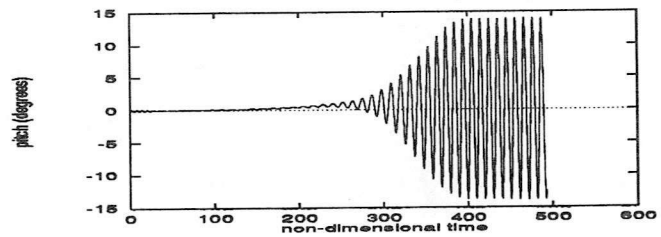

$\overline{U}$=2.0

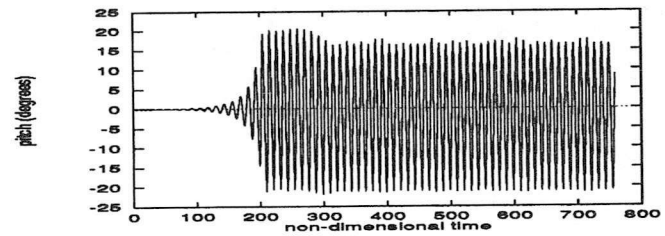

$\overline{U}$=2.2

Figure 6. *Pitch response for varying $\overline{U}$ at Mach 0.85 on 150x30 mesh, far field at 20c and 150 steps/pitching cycle.*

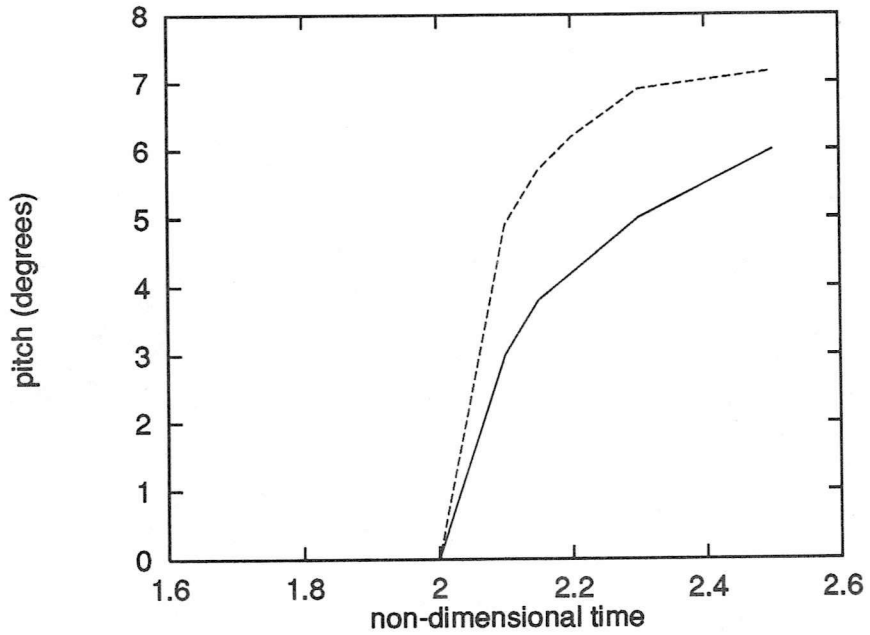

Figure 7. *Comparison of limit cycle amplitudes at Mach 0.92 - solid line present results, dashed line from Bendiksen and Kousen.*